Pergamon

0956-7151(95)00144-1

Acta mater. Vol. 44, No. 1, pp. 367–381, 1996
Elsevier Science Ltd

1359-6454/96 $15.00 + 0.00

ON THE NATURE OF LOW TEMPERATURE INTERNAL FRICTION PEAKS IN METALLIC GLASSES†

V. A. KHONIK[1]‡ and L. V. SPIVAK[2]

[1]Department of General Physics, State Pedagogical University, Lenin Street 86, Voronezh 394043 and [2]State University, Bukireva 15, Perm 614600, Russia

(Received 9 November 1992; in revised form 15 February 1995)

Abstract—Low temperature ($30 < T < 300$ K) internal friction in a metallic glass $Ni_{60}Nb_{40}$ subjected to preliminary inhomogeneous deformation by cold rolling, homogeneous tensile deformation or electrolytic charging with hydrogen is investigated. Cold rolling or hydrogenation result in appearance of similar internal friction peaks and hysteresis damping. Homogeneous deformation has no influence on low temperature internal friction. The phenomenon of microplastic deformation during hydrogenation of weakly stressed samples is revealed. It is argued that microplastic deformation of metallic glasses during hydrogenation without external stress takes place too. Plastic flow both on cold rolling and hydrogenation occurs via formation and motion of dislocation-like defects which are the reason of the observed anelastic anomalies. It is concluded that low temperature internal friction peaks described in the literature for "as-cast", cold deformed and hydrogenated samples have common dislocation-like origin.

1. INTRODUCTION

The internal friction (IF) method is very powerful for investigation of structure and properties of solids and often gives information which cannot be obtained otherwise. In the course of the last 10–15 yr this method was being applied to investigations of metallic glasses (MG) intensively and in a number of cases interesting results were obtained. In the present paper we discuss the nature of relaxation IF peaks which can be observed below the room temperature in MG different both by chemical composition and technology of fabrication. Depending on the character of preliminary treatment of samples the observed IF peaks [1–30] can be divided into three groups. In the papers [1–8] samples underwent no preliminary treatment and IF was measured in the as-prepared condition. The authors of these papers either frame no hypothesis about the origin of these peaks or assume their connection with structure defects of some kind. In the papers [9–24] specimens (containing hydride-forming elements or without them) were hydrogenated either electrolytically or from the gaseous phase. It is argued in these papers that the observed IF peaks are a result of Snoek-type hydrogen relaxation. At last, in the papers [25–30] specimens were subjected to preliminary cold plastic deformation which resulted in slip band formation. The IF peaks observed after such a treatment were interpreted in the framework of dislocation ideas about MG inhomogeneous plastic flow and the corresponding relaxation process was considered to be an analog of the Hasiguti relaxation in crystals.

It should be emphasized that IF peaks observed in all three cases mentioned above are considerably similar. On the IF temperature dependence there appears either one wide peak, which can be asymmetrical, or (rarely) two peaks. The IF peak temperature is in the range 150–250 K, the IF peak height—$5 \cdot 10^{-3}$ to 10^{-2}, the activation energy—0.3 to 0.5 eV, the frequency factor is about the Debye frequency and the corresponding modulus deficiency is 5–15%. Proceeding from the shape, temperature and activation parameters of the IF peaks it is impossible to determine what preliminary treatment was used. For example, the IF peaks in hydrogenated $Pd_{77,5}Cu_6Si_{16,5}$ described in [12] are similar, taking into account the difference in frequencies used, to the IF peak in the same MG deformed by cold forging [25]. The IF peaks in hydrogenated [19] and cold rolled [26, 28] $Cu_{50}Ti_{50}$ are practically identical. The IF peak in $Ni_{78}Si_8B_{14}$ in the initial state [7] is very similar to the IF peak in the same MG after cold rolling [27, 28]. The similarity of IF peaks in as-cast and hydrogenated conditions was pointed out in [10].

The above-mentioned leads naturally to the proposal that the IF peaks under consideration (there are no other IF peaks in MG in the range $30 < T < 300$ K at frequencies $< 10^4$ Hz) have the same origin because it is evident that Snoek relaxation due to light hydrogen atoms can result in formation of the IF peak which must be very different from that caused by motion of point-like or line

†Dedicated to the memory of Professor A. M. Rotschupkin.
‡To whom all correspondence should be addressed.

structure defects. To clarify this situation we measured low temperature IF in cold rolled and hydrogenated samples under identical experimental conditions. $Ni_{60}Nb_{40}$ metallic glass was chosen as an example. The obtained results allowed us to conclude that hydrogen is only an indirect reason of IF peak formation and the direct reason consists of microplastic deformation of structure during hydrogenation. Besides that, it was determined that deformation-induced IF peak at definite conditions can be very sensitive to small plastic deformation and it is impossible without special experimental efforts to determine whether the IF peak is typical for as-cast specimens.

2. EXPERIMENTAL

$Ni_{60}Nb_{40}$ ribbon obtained by usual melt spinning technique was used for investigations. Ribbon thickness and width were 40–50 μm and 1–2 mm, respectively. X-ray diffraction and transmission electron microscopy (TEM) were performed to ensure the ribbon to be entirely amorphous. IF was measured by using the vibrating reed technique. Samples were clamped at one end with a free length of 3–10 mm and excited electrostatically. IF was calculated as $Q^{-1} = k/N$, where N is the number of free specimen vibrations corresponding to a definite lowering of their amplitude, k is the apparatus constant. Error limits of IF measurements were about 8–9% at IF level $\approx 10^{-2}$ and 1–2% at $Q^{-1} \approx 10^{-4}$. Our experimental apparatus permitted determination of strain tensile amplitude ϵ_0 during flexural vibrations. The corresponding experimental details are described in [27]. ϵ_0 was varied in the range $3 \cdot 10^{-7}$–$1 \cdot 10^{-4}$. ϵ_0 error limits were 40–50% near the borders and about 15% in the middle of this range. The measurements were performed under vacuum $\approx 10^{-3}$ torr at temperatures ranging from 30 to 300 K and frequencies varying from 200 to 3000 Hz. A temperature step of the measurements was equal to 2 K. A change of vibration frequency was carried out by shortening of the same specimen. All IF temperature dependences at various strain amplitudes, frequencies and after heat treatments were measured without withdrawal of samples from the clamp in order to preserve them from uncontrolled deformations which arise at every new gripping.

The specimens were predeformed using the rolling mill analogous to that described in [31]. Thickness decrease of ribbon due to one rolling cycle was about 0.5–1%. The prestrain value ϵ_p was estimated as the average value of the relative thickness decrease and the relative length increase.

Electrolytic hydrogenation was performed in 1 N H_2SO_4 + 100 mg/l As_2O_3. The hydrogenation temperature under the cathode current densities used

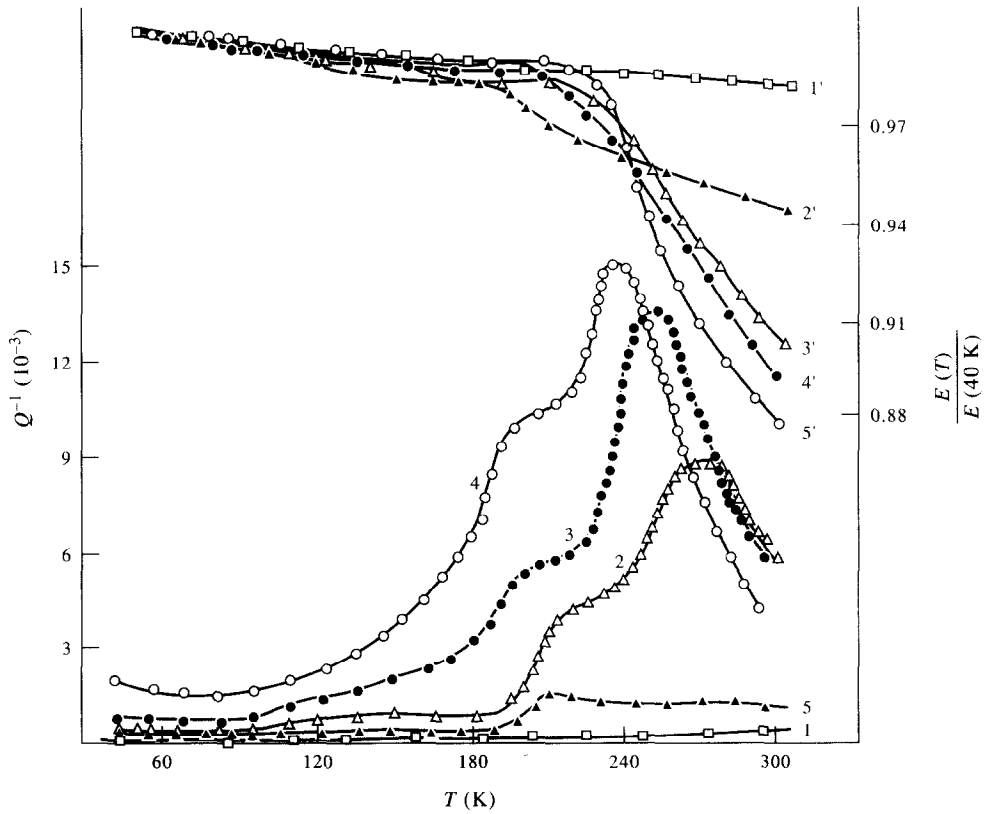

Fig. 1. Temperature dependences of IF (1–5) and normalized elastic modulus (1′–5′) at frequencies ≈ 300 Hz in the as-cast state at $\epsilon_0 = 1 \cdot 10^{-5}$ (1, 1′); after 3% rolling at: $\epsilon_0 = 7 \cdot 10^{-6}$ (2, 2′), $\epsilon_0 = 3 \cdot 10^{-5}$ (3, 3′), $\epsilon_0 = 5 \cdot 10^{-5}$ (4, 4′); after 12% rolling at $\epsilon_0 = 1.6 \cdot 10^{-5}$ (5, 5′).

($J = 2$ and 10 mA/cm^2) was about 293 K. Platinum wire-net served as an anode. Deformation of samples during hydrogenation was investigated under tensile or torsion creep conditions with the help of specially constructed testing machines. In both cases the sample gauge length was equal to ≈ 50 mm and the sample width was about 1 mm. Elongation and twist angle relative errors were about $5 \cdot 10^{-4}$ and $5 \cdot 10^{-5}$, respectively. The samples used for these investigations were etched in 50% HNO_3 during 1 min before testing in order to remove surface oxidized layer.

3. RESULTS AND DISCUSSION

3.1. Internal friction in cold rolled $Ni_{60}Nb_{40}$

Temperature dependences of IF (Q^{-1}) and normalized elastic modulus (E) in the as-cast state and after cold rolling are shown in Fig. 1. After careful gripping of as-cast specimen $Q^{-1}(T)$ and $E(T)$ have no peculiarities: IF weakly increases and E weakly decreases with temperature rise (curves 1, 1′). Rolling by $\epsilon_p = 2$–4% results in appearance of large IF peaks [Q^{-1}_{max} can reach $(1$–$3) \cdot 10^{-2}$] with the corresponding modulus deficiency of about 10–12% (curves 2, 2′–4, 4′). The shape of the peak is quite well reproducible on repeated temperature scans of the same sample at fixed frequency f and strain amplitude ϵ_0. However, for various samples predeformed by the same ϵ_p the shape of the peak can differ significantly. In the majority of cases one can observe a wide asymmetric peak which can have a low temperature shoulder (Fig. 1). Sometimes this shoulder transforms into a separate IF peak (see below, Fig. 5). The character of the IF temperature dependence is

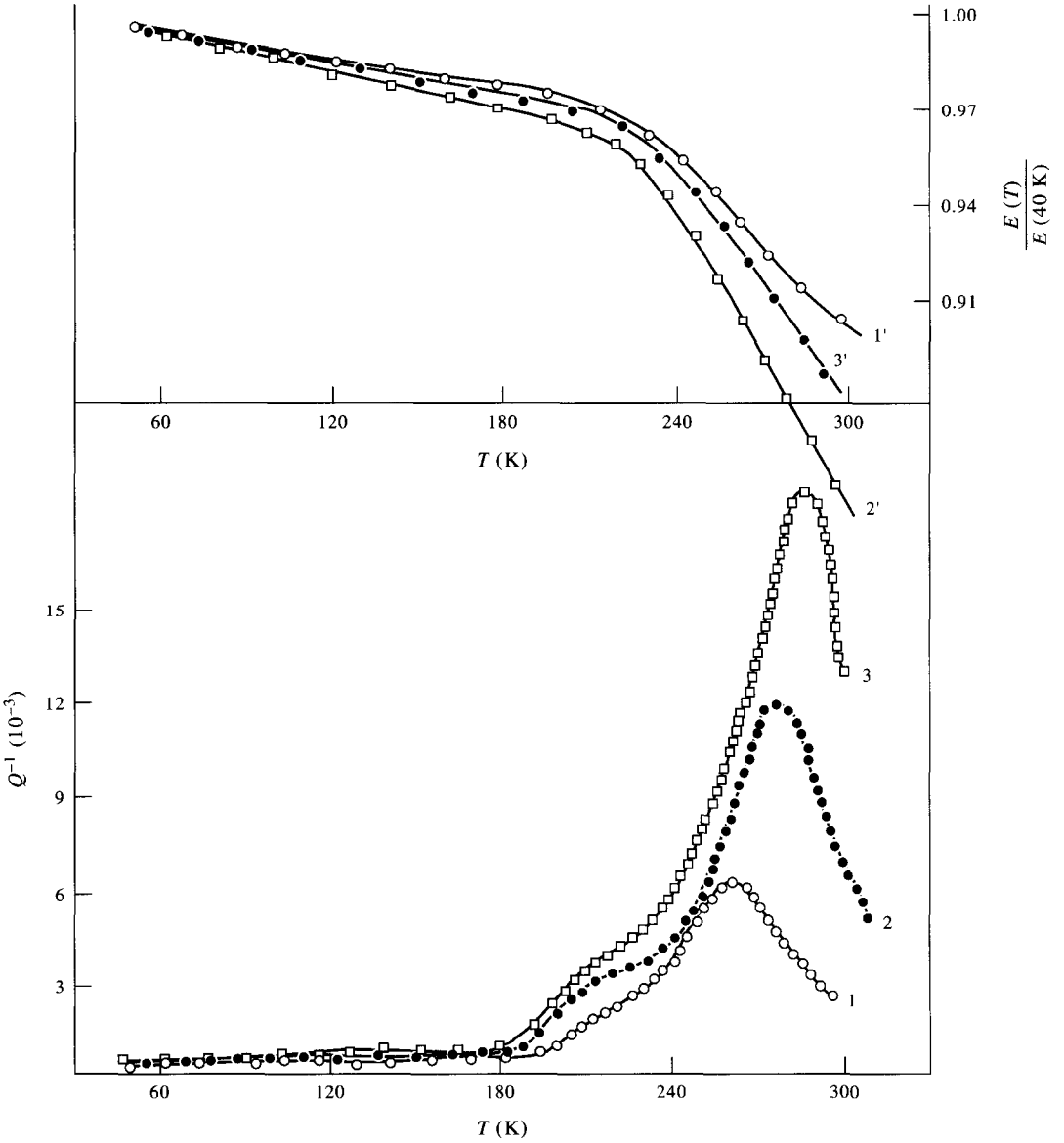

Fig. 2. Temperature dependences of Q^{-1} (1–3) and E (1′–3′) after 3% rolling at frequencies 309 Hz (1, 1′), 703 Hz (2, 2′), 1440 Hz (3, 3′). $\epsilon_0 = 2.5 \cdot 10^{-5}$.

strongly dependent on ϵ_0, ϵ_p and f. An increase of ϵ_0 at fixed ϵ_p and f results in a peak height rise and in a peak shift to low temperatures by 30–40 K on a tenfold ϵ_0 increase (curves 2–4, Fig. 1). Simultaneously, the damping level at temperatures below the IF peak (at $T < 150$ K) increases significantly. On subsequent predeforming the IF peak height decreases (curve 5, Fig. 1) and in heavily deformed samples $Q^{-1}(T)$ and $E(T)$ are close to those in the as-cast state. An increase of f at fixed ϵ_p and ϵ_0 results in IF peak shift to high temperatures and in its height increase. However, low temperature damping remains almost unchanged (Fig. 2). Joint consideration of the Figs 1 and 2 leads to the conclusion that IF in deformed samples has a compound character: at $T < 150$–180 K IF is mainly hysteresis (frequency independent) and at 180 K $< T <$ 300 K hysteresis IF is superimposed by the relaxation-type IF peak. It must be noted also that IF is amplitude-independent in as-cast specimens and predeforming results in strong IF amplitude dependence.

The logarithm of the vibration frequency vs the inverse IF peak temperature is shown in Fig. 3, curve 1. The activation parameters calculated from this dependence are: activation energy $U = 0.51$ eV, pre-exponential factor $\tau_0 = 1 \cdot 10^{-13}$ s.

The deformation-induced IF peak is stable on prolonged ageing at room temperature: 5–6 month exposure has no significant influence on $Q^{-1}(T)$. However, the IF peak disappears after moderate heat treatment. It is seen from Fig. 4 that the IF peak and the corresponding modulus deficiency formed by prestraining ($\epsilon_p = 2.5\%$) disappear almost completely after ageing at $T_a = 523$ K for 15 min (crystallization beginning temperature of the MG under investigation is about 915 K at $\dot{T} = 10$ K/min). Repeated predeforming restores the IF peak (Fig. 4, curve 3).

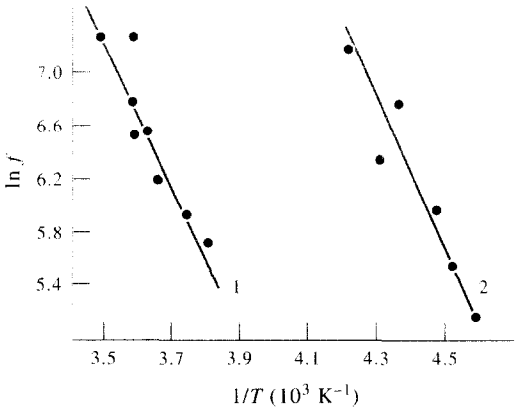

Fig. 3. The logarithm of the vibration frequency vs the inverse IF peak temperature for rolled (1) and hydrogenated (2) samples.

Figure 5 illustrates the influence of 2 MeV electron irradiation on $Q^{-1}(T)$ and $E(T)$ of a predeformed sample. The experiment was carried out as follows. After predeforming and performing measurements (their results are given by curves 1, 1′) the sample together with the clamp was irradiated with an electron beam. Exposure dose and source intensity were $1 \cdot 10^{18}$ cm^{-2} and $2 \cdot 10^{14}$ cm^{-2} s^{-1}, respectively. In order to limit specimen heating during irradiation water cooling was used. As is seen from curves 2, 2′ irradiation results in almost complete disappearance of deformation-induced IF peak and corresponding modulus deficiency.

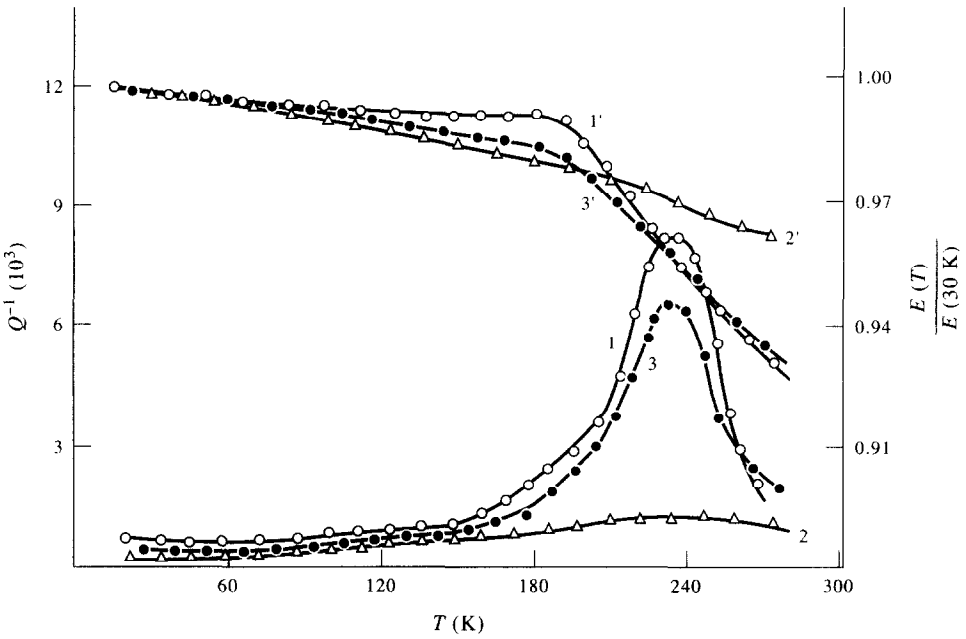

Fig. 4. Temperature dependences of Q^{-1} (1–3) and E (1′–3′) at frequencies ≈ 300 Hz and $\epsilon_0 = 1.6 \cdot 10^{-5}$ after 2.5% rolling (1, 1′) and subsequent annealing at 523 K during 15 min (2, 2′) followed by 1% rolling (3, 3′).

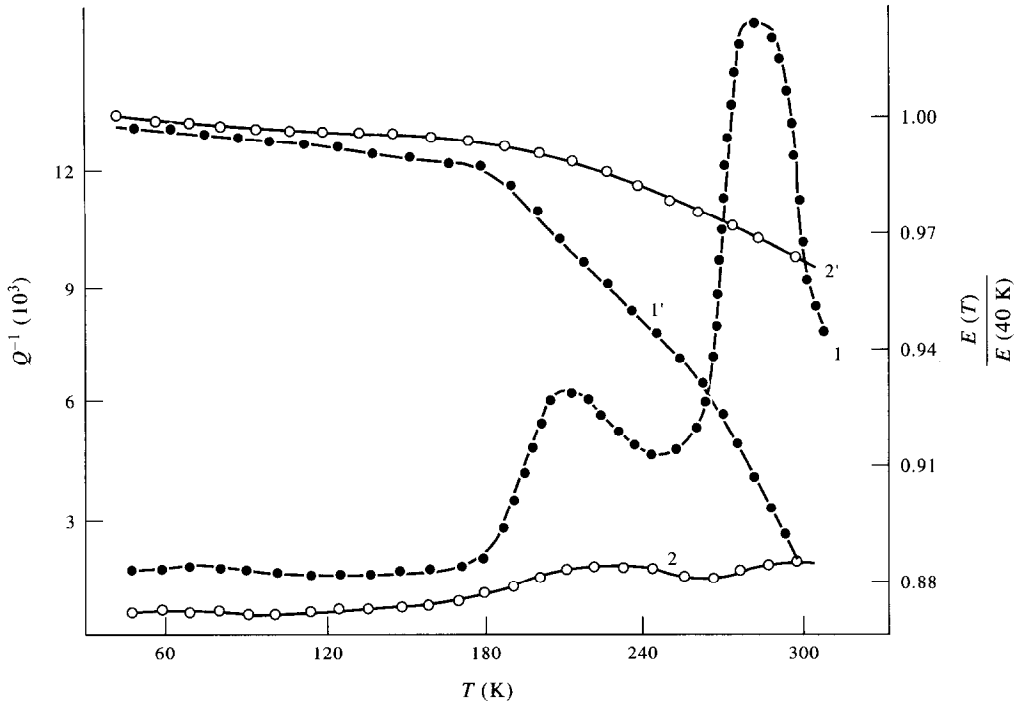

Fig. 5. Influence of 2 MeV electron irradiation on the deformation-induced IF peak: temperature dependences of Q^{-1} (1, 2) and E (1′,2′) at frequencies ≈ 300 Hz and $\epsilon_0 = 7 \cdot 10^{-5}$ after 2.5% rolling (1, 1′) followed by $1 \cdot 10^{18}$ cm^{-2} irradiation dose (2, 2′).

3.2. On the nature of anelastic anomalies in rolled samples

First of all it must be noted that deformation-induced IF peaks considered above are quite analogous to those in other cold-worked MG based on Cu–Ti, Ni and Pd [25–30]. The present authors have observed also analogous IF peaks in a number of Fe–Ni and Co-based MG. Therefore, one can suppose that appearance of IF peaks after inhomogeneous deformation by rolling is a phenomenon that is typical for MG.

A sharp change of MG anelastic properties after rolling clearly indicates a significant modification of internal defect structure. A natural question about the character of defects responsible for this change should be raised. We believe that the obtained results corroborate the dislocation concept [25–30, 32–41] of MG inhomogeneous plastic flow. In our opinion, at present this concept provides the most plausible picture of localized deformation of amorphous structures.

The first point for this statement results from the fact of the presence of the hysteresis damping in predeformed samples. As it is generally known [42], hysteresis damping in non-ferromagnetic and non-phase-transforming crystals is a typical dislocation effect and in the sonic range is due to breakaway of dislocations from point obstacles. In non-dislocated crystals (whiskers) hysteresis damping is absent [43]. Therefore, the amplitude independent character of the IF in as-cast samples can be a result of absence of (mobile) dislocation-like defects in structure. Preliminary deformation results in formation of such defects and their motion in external alternating stress fields leads to the appearance of hysteresis damping and relaxation IF peak. The established similarity [25, 30] of IF amplitude dependences in deformed amorphous and crystalline states seems to be very indicative in this sense. It should be mentioned also that an attempt to explain amplitude dependent damping as a result of point-like defect motion will entail considerable difficulties. In particular, if one supposes such a possibility, it becomes unclear why any IF amplitude dependence is absent in the initial state which is characterized definitely by a considerable point-like defect density.

A characteristic feature of deformation IF peaks in MG consists of the possibility of their disappearance as a result of high prestrain or irradiation. An analogous situation takes place for low temperature IF peaks in deformed crystals [42] and this fact is one of the most striking evidences of their dislocation nature. Locking of dislocation-like defect motion in MG due to either internal stress increase at high prestrain or formation of irradiation point-like defects is a probable reason for disappearance of anelastic anomalies mentioned above. The possibility of the IF peak height decrease on predeforming clearly indicates the "non-point-like" character of inhomogeneous flow defects because in the opposite case (flow by formation and motion of point-like defects) one should expect only an increase of the IF peak height on predeforming.

The other fact which definitely corroborates the concept under consideration originates from lowering of the IF peak temperature with an increase of the deformation amplitude ϵ_0 (Fig. 1, curves 2–4). In the case of point-like defect relaxation the deformation amplitude has no effect on the peak temperature because such a relaxation is characterized by a small activation volume V and the effective activation energy U_{eff} is independent of the applied shear stress σ_s. If the relaxation mechanism includes motion of line defects with high activation volume, the effective activation energy decreases as $U_{\text{eff}} = U_0 - \sigma_s V$ ($U_0 = \text{constant}$). A decrease of the activation energy at a fixed frequency means lowering of the corresponding IF peak temperature. Such a situation is realized in the case of dislocation relaxations in crystals [44].

Let us evaluate the activation volume of relaxation. A relaxation maximum takes place under the condition $\omega\tau = 1$, where $\omega = 2\pi f$ is the circular frequency, $\tau = \tau_0 \exp((U_0 - \sigma_s V)/kT)$ is the relaxation time. If measurements are carried out at two various shear deformation amplitudes, σ_{s1} and σ_{s2} ($\sigma_{s1} < \sigma_{s2}$), the corresponding peak temperatures are equal to T_1 and T_2 ($T_1 > T_2$). It is easy to show that

$$V = \frac{U_0(T_1 - T_2)}{T_1\sigma_{s2} - T_2\sigma_{s1}}. \tag{1}$$

Shear deformation amplitude can be determined from Hooke's law: $\sigma_s = \epsilon_0 E/\sqrt{3}$, where ϵ_0 is the tensile deformation amplitude, E is the Young's modulus. Taking $E = 109$ GPa [39], $\epsilon_{01} = 7 \cdot 10^{-6}$, $\epsilon_{02} = 5 \cdot 10^{-5}$, $T_1 = 270$ K, $T_2 = 235$ K (see curves 2–4 in Fig. 1), $U_0 = 0.51$ eV we get $V = 3.8$ nm^3. In the b^3-units (b is the average interatomic distance which is equal to 0.263 nm for $Ni_{60}Nb_{40}$ [45]) $V \approx 210$ and in the Ω-units (Ω is the average atomic volume)—approximately twice greater. Such a large value of the activation volume contradicts the assumption about the point-like character of defects responsible for relaxation but appears to be an argument for the dislocation flow mechanism. It should be noted also that the V-value obtained coincides within an order of magnitude with the activation volume value evaluated from the stress relaxation data in the same MG at room temperature [39]. Values of $V \approx 100\, b^3$ are characteristic of dislocation relaxations in crystals at low temperatures [46].

3.3. Effect of homogeneous deformation on low temperature damping

The dislocation-like character of inhomogeneous deformation at room temperature, in our opinion, is determined by the fact that the structural relaxation rate at this temperature is very low and elementary shear events are correlated therefore [47]. On the other hand, homogeneous plastic flow occurs under the condition of intensive structural relaxation and it can be represented as a totality of uncorrelated shear events [41, 47,48]. If such a viewpoint is correct and if dislocation-like defects which arise on inhomogeneous deformation are responsible for low temperature IF anomalies, one can conclude that homogeneous flow must have a considerably different effect on low temperature damping. Our experiment confirmed this proposal. The corresponding results are shown in Fig. 6.

A sample was plastically deformed by tension at $T_a = 773$ K. The choice of this temperature was determined by the necessity of prestraining by 4–6% that is impossible at lower temperatures. Plastic flow at T_a and at the strain rate chosen is completely homogeneous [47]. After deformation by $\epsilon_p = 1.8\%$ the sample was cooled down in the stressed state to room temperature, extracted from the testing machine, shortened and after that it was carefully gripped in the Q^{-1}-measuring apparatus. $Q^{-1}(T)$ and $E(T)$ after such a treatment are given by curves 0 and 0′ in Fig. 6(b). As it is seen, an IF peak with the corresponding modulus deficiency is observed. However, more thorough investigations have shown that the appearance of this peak is an experimental artifact due to deformation of sample during gripping in the Q^{-1}-apparatus.

To show this, the specimen 1 was gripped in clamp 2 of the Q^{-1}-apparatus, the clamp was fastened in the tensile testing machine [Fig. 6(c), lower part], plastically deformed by 1.8, 4 or 6% [points 1–3 in the σ–ϵ diagram, Fig. 6(a)] and cooled down in the stressed state to room temperature. Then the clamp with the specimen was taken out from the testing machine, the specimen was shortened without extracting from the clamp [Fig. 6(c), upper part] and after that the clamp was fastened in the Q^{-1}-apparatus. This method allowed the avoidance of additional uncontrolled straining during re-gripping of sample. The results are given by curves 1–4 and 1′–4′ in Fig. 6(b). It is seen that homogeneous deformation has no effect on low temperature dependences of IF and elastic modulus: $Q^{-1}(T)$ and $E(T)$ in deformed or simply aged (at T_a) states are completely identical.

The obtained results suggest that the mechanisms of inhomogeneous and homogeneous flow are quite different. Homogeneous flow is not accompanied by formation of new structural defects and does not change, therefore, the dissipative properties of the material. Inhomogeneous flow results in formation of new dislocation-like defects, not characteristic of the initial state, which determine the anelastic anomalies considered above. Besides that, one can conclude that low temperature IF can be extremely sensitive to small plastic strains which can arise in course of sample gripping (see also [27, 28]). We believe that low temperature IF peaks in the "initial" state described in [1 8] are due to plastic deformation of samples during gripping.

Plastic deformation can occur also during hydrogenation of samples resulting in appearance of the anelastic anomalies which are almost completely analogous to those described above.

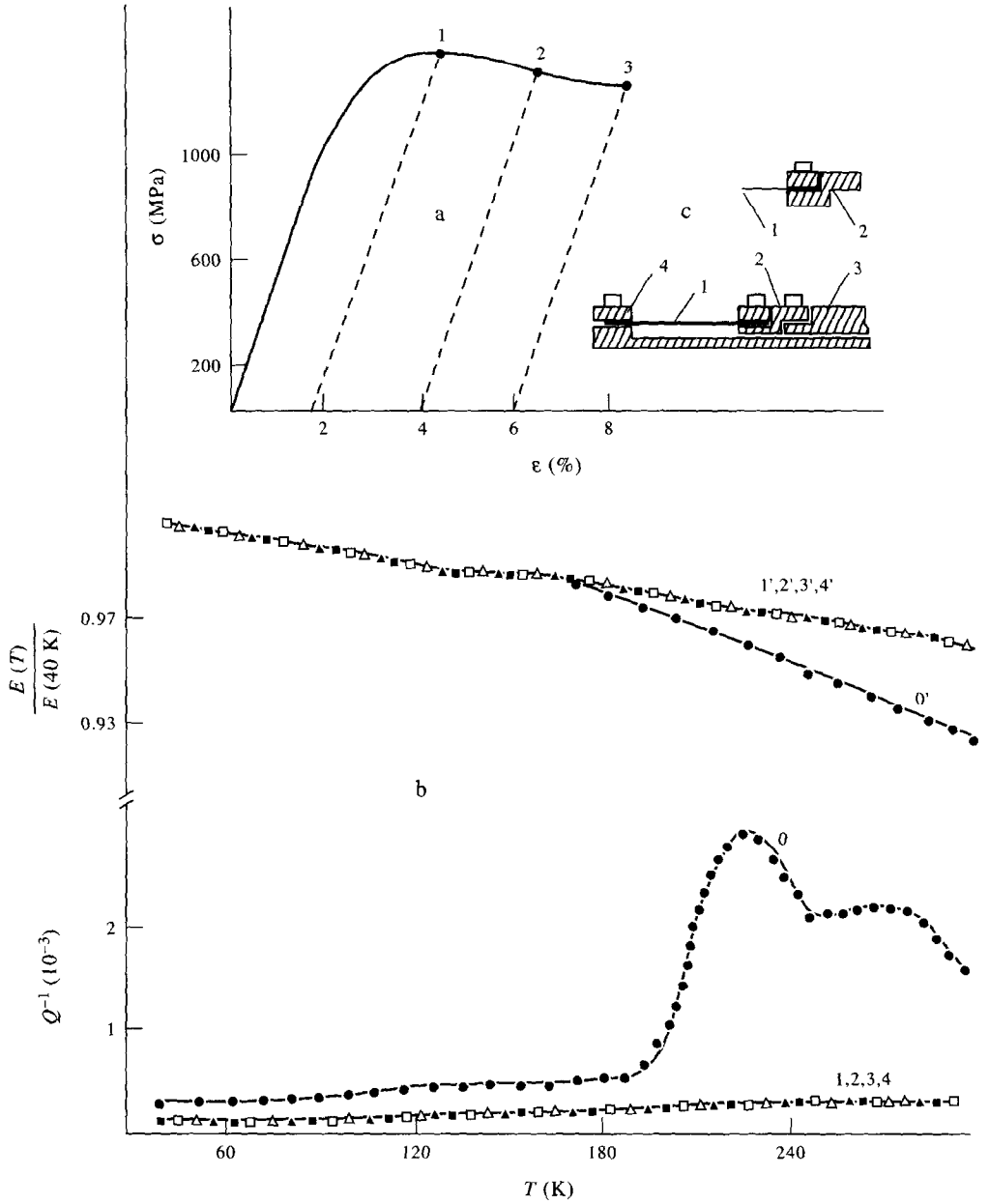

Fig. 6. Influence of homogeneous deformation on low temperature IF: stress vs tensile deformation at $T = 773$ K and $\dot{\epsilon} = 5 \cdot 10^{-5}$ s^{-1} (a); temperature dependences of Q^{-1} and E after homogeneous tensile deformation by 1.8% and extraction of sample from the clamp (0,0′), after deformation (1–3, 1′–3′) by 1.8, 4 or 6% (points 1–3 in the σ–ϵ diagram) or ageing at $T = 773$ K during 20 min (4, 4′) without extraction of samples from the clamp (b) that is illustrated in (c) (1: specimen; 2: clamp; 3, 4: grips of the tensile testing machine).

3.4. Deformation and internal friction of hydrogenated $Ni_{60}Nb_{40}$

3.4.1. Hydrogenation-induced microplasticity. First of all the phenomenon of MG microplastic deformation during hydrogenation should be considered.

$Ni_{60}Nb_{40}$ samples were placed in the electrolytic cell, loaded by a constant tensile stress and tensile elongation was measured during subsequent hydrogenation. Figure 7(a) shows the kinetics of the deformation increment $\Delta l/l$ (l is the length of loaded sample without hydrogenation. Δl is the length increment during hydrogenation in the stressed state) up to fracture of samples during hydrogenation at two various stresses and polarization current densities. It is seen that hydrogenation of weakly stressed samples results in sufficient deformation increment (up to 1–2%) which can be ten or more times greater than the preceding elastic deformation and is comparable with the fracture deformation ($\approx 2.2\%$ [39]) at room temperature without hydrogenation. The deformation increment rate and time before fracture are

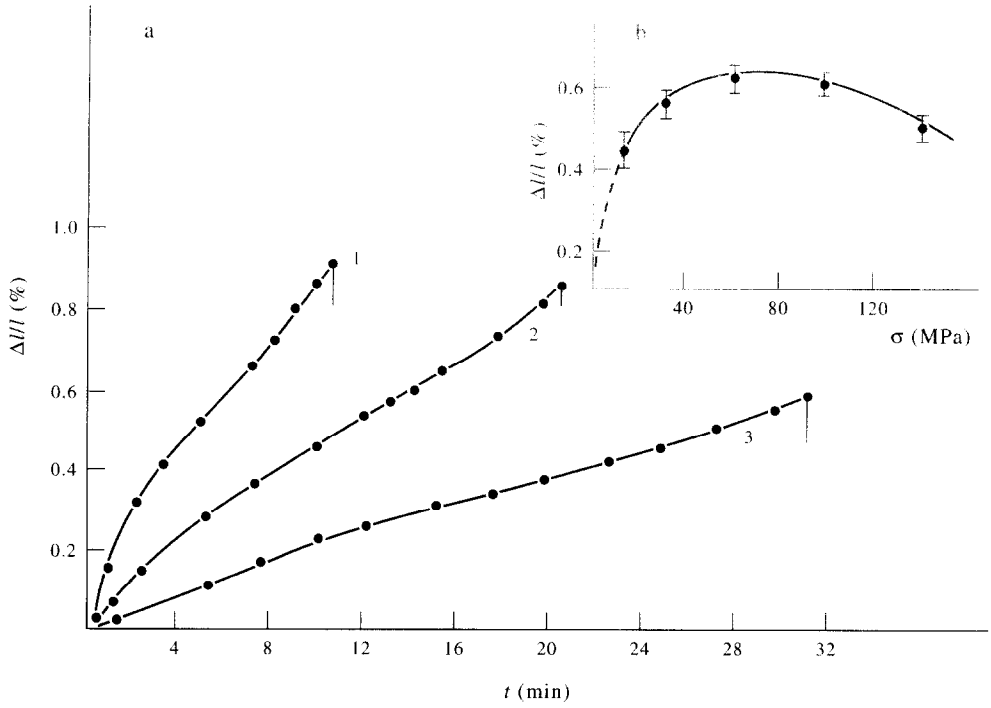

Fig. 7. Hydrogenation-induced tensile creep. (a) Relative elongation kinetics during hydrogenation under applied stress 145 MPa (1, 3) and 14.5 MPa (2). Current densities: 10 mA/cm^2 (1, 2) and 2 mA/cm^2 (3). (b) Relative elongation after 25 min hydrogenation vs applied stress, $J = 2$ mA/cm^2.

strongly dependent on the applied stress, hydrogenation current density, fluctuations of MG composition and quenching rate, variations of electrolyte composition and temperature, time of preliminary chemical surface etching of samples. A decrease of the current density under other fixed conditions results in a lowering of the deformation increment rate and in simultaneous increase of time before fracture. The dependence of the deformation increment on the applied stress at a constant hydrogenation time and current density is complex [Fig. 7(b)]. At low σ (< 50 MPa) the deformation increment goes down with decrease in σ at any t (we were not able to carry out the experiments at $\sigma < 5$ MPa due to low stiffness of samples). At high σ used a decrease of $\Delta l/l$ with σ was observed most often, but sometimes the reverse dependence was registered, depending, obviously, on uncontrolled experimental conditions.

The results of analogous experiments under torsion are shown in Fig. 8. After loading by the torque M and switching on the polarization current an increment of the torsion angle is observed. The torsion deformation increment $\Delta\varphi/\varphi$ (φ is the twisting angle of a loaded sample, $\Delta\varphi$ is the increment of this angle during hydrogenation in the stresses state) can reach 1.5–2.5. Analogously to the case of tensile loading an increase of J results in increasing of deformation at a fixed hydrogenation time, but the time before fracture decreases. The dependence $\Delta\varphi/\varphi$ vs M at a constant t and J, as different from the case of tension, is quite unique: an increase of torque always results in a lowering of the deformation increment [Fig. 8(b)] and in a decrease of time before fracture [Fig. 8(a)]. Due to apparatus constraints we failed to carry out the experiments at $M < 2 \cdot 10^{-4}$ Nm.

It must be noted that in all cases turning off the polarization current leads to immediate stoppage of the deformation increment and any relaxation within experimental resolution during several hours is absent. Switching on the current restores the deformation increment rate instantly.

Hydrogenation in the stressed state results in irreversible deformation of samples. This conclusion follows from the unloading experiments of hydrogenated samples. The corresponding results for tension are shown in Fig. 9. The arrows above the curves indicate switching on ($\uparrow$) and switching off ($\downarrow$) the polarization current with simultaneous loading and unloading of samples. The first loading–unloading cycle without hydrogenation illustrates reversibility of the elastic deformation. After that at $t = 0.3$ min the sample was loaded by $\sigma = 145$ MPa and the polarization current was turned on. Joint action of stress and hydrogenation during the subsequent time interval $\Delta t \approx 0.7$ min results in the deformation increment. At $t = 1$ min the polarization current was switched off and the sample was unloaded down to $\sigma \approx 5$ MPa. However, the initial length of the sample was not restored and any strain recovery within experimental resolution was absent. Then the sample was loaded by the same stress afresh, the hydrogenation current was turned on and the outlined procedure was repeated several times. The results of the experiment indicate an accumulation of the

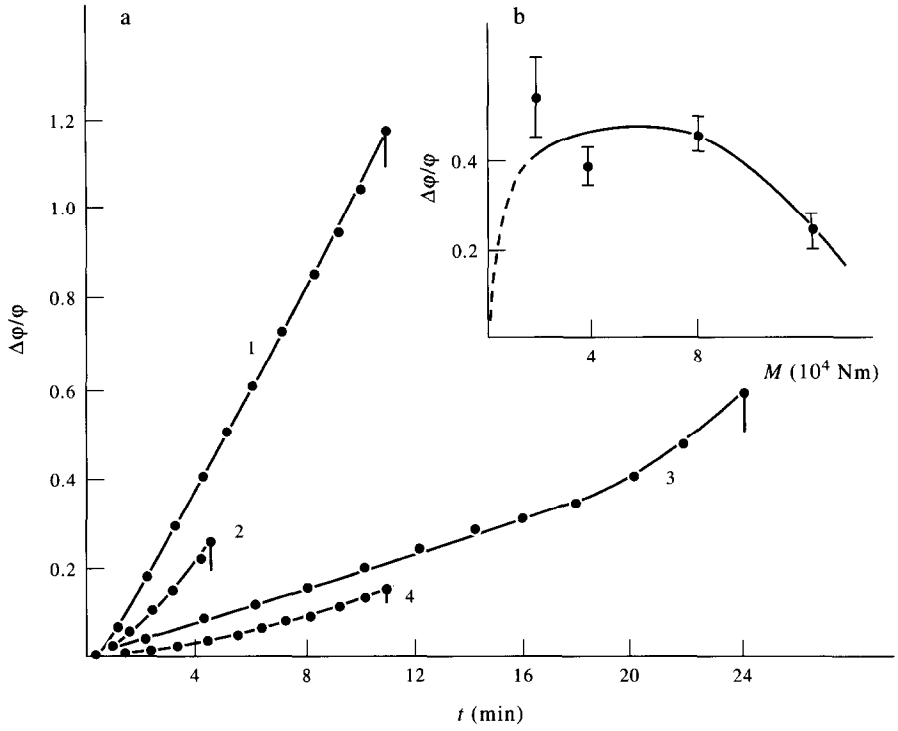

Fig. 8. Hydrogenation-induced torsion creep. (a) Torsion kinetics during hydrogenation under applied torque $4 \cdot 10^{-4}$ Nm (1, 3) and $12 \cdot 10^{-4}$ Nm (2, 4). Current densities: 10 mA/cm^2 (1, 2) and 2 mA/cm^2 (3, 4). (b) Torsion deformation after 4 min hydrogenation vs applied torque, $J = 10$ mA/cm^2.

irreversible deformation after hydrogenation in the stressed state. Analogous data were obtained for torsion.

Hydrogen dissolution results in the volume expansion of a metal. One can raise a question about the origin of the deformation described above: either this deformation is due to the volume expansion or it is conditioned mainly by an activation of the microplastic deformation processes during hydrogenation. The volume expansion value can be represented as [49] $\Delta V/V = c\Delta v/\Omega$, where c is the atomic hydrogen concentration, Δv is the volume change per hydrogen atom, Ω is the mean volume per atom. The characteristic Δv-value for MG is equal to $\approx 2.6 \cdot 10^{-3}$ nm^3 [50]. Our measurements of the hydrogen concentration carried out by the vacuum melting method for the samples hydrogenated by $J = 10$ mA/cm^2 during 40 min gave $c = 2.6$ at.%. Then setting for $Ni_{60}Nb_{40}\Omega \approx b^3 = 1.82 \cdot 10^{-2}$ nm^3 (see above) one can evaluate linear expansion of a sample after hydrogenation under $J = 10$ mA/cm^2, $t = 20$ min as $\Delta l/l \approx \Delta V/3V = 1.3 \cdot 10^{-2} \cdot 2.6 \cdot 10^{-3}/3 \cdot 1.82 \cdot 10^{-2} \approx 6 \cdot 10^{-4}$. However, the measurements of deformation under hydrogenation [Fig. 7(a), curve 2] give a significantly higher value: $\Delta l/l \geqslant 8 \cdot 10^{-3}$. Therefore, one can suppose that the volume expansion cannot explain the observed elongation. An analogous conclusion can be drawn from the fact that at the same hydrogen injection rate the deformation increment rate can be decreased with the applied stress rise [Fig. 7(b), Fig. 8(b)]. If one supposes pure volume expansion then such a dependence should be absent.

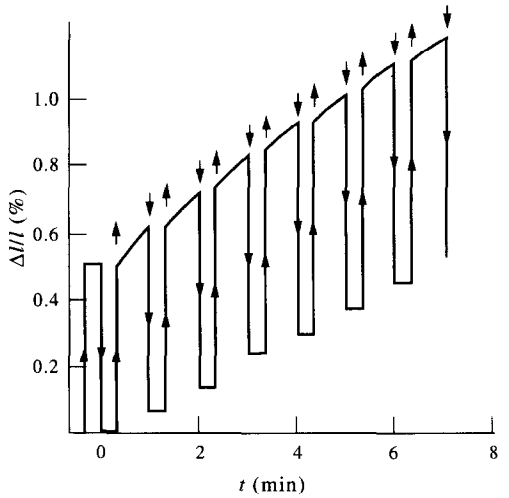

Fig. 9. Tensile elongation kinetics under cycle loading and hydrogenation. The arrows above the curves indicate: time moments of loading and switching on (↑) the hydrogenation current, time moments of unloading and switching off (↓) the hydrogenation current. $\sigma = 145$ MPa, $J = 10$ mA/cm^2.

However, the most convincing fact which indicates that the volume expansion does not play any key role in the phenomenon discussed consists of the presence of the hydrogen-induced torsion creep. The torsion angle of a sample loaded by the torque M is equal to [51]: $\varphi = GMl/ba^3$, where G is the constant which

includes the shear modulus, l is the sample length, a is the narrow side and b is the wide one of a sample with rectangular cross-section. Regarding the elastic modulus to be weakly dependent on hydrogen concentration [52] and the volume expansion to be isotropic ($da/a \approx db/b \approx dl/l$), for the case $M = \text{constant}$ one can obtain $d\varphi/\varphi = -3da/a$. Because $da > 0$ under hydrogenation, it must be concluded that $d\varphi < 0$ and *the volume expansion decreases the torsion angle* whereas the experimental fact consists of an increase of this angle, towards the applied torque. Therefore, volume expansion is not the reason of the hydrogen-induced torsion creep. The similarity of the observed effects under various loading modes and the arguments mentioned above indicate that this conclusion is valid also in the case of tension.

Hence, the points concerned above allow one to conclude that the hydrogen-enhanced deformation originates from an activation of microplastic flow of structure during hydrogenation.

It should be mentioned that this effect is not unexpected because such a behaviour is known for crystalline metals. For the first time the hydrogen-induced activation of tensile creep was observed by Hagi *et al.* [53] and Park *et al.* [54] in α-Fe. The investigations [53–55] have shown that the hydrogenation-induced elongation is conditioned by an activation of dislocation sources and facilitation of dislocation motion. Spivak *et al.* observed sharp acceleration of torsion creep during hydrogenation of α-Fe and of a number of other (including hydride-forming) metals (see [56–59] and references in [59]). The investigations of structure and properties of hydrogenated crystalline metals indicate an activation of dislocation deformation and an increase of dislocation density due to: (i) an internal stress rise as a result of molecular hydrogen accumulation in voids and cracks under high pressure (up to 10^2–10^3 MPa) [60–63]; (ii) an internal stress rise due to the difference between the specific volumes of matrix and growing hydrides [59]; (iii) a weakening of interionic metal–metal bonding as a result of hydrogen adsorption [61]. There are no grounds to consider that these effects are absent in the case of metallic glasses and, therefore, it can be supposed that hydrogenation-induced microplasticity is caused by the same reasons.

We observed this effect in a number of MG either containing hydride-forming elements or without them and, thus, it can be assumed that this effect is characteristic of MG.

As pointed out above, the hydrogenation-induced microplasticity is observed under influence of small stresses, about several percents of the fracture stress. Internal quenching stresses in MG are of similar magnitude [64] and, therefore, one can expect that plastic deformation of structure under hydrogenation without external stress will occur also, resulting in generation of dislocation-like defects. Motion of these defects in an external alternating stress field can lead to the appearance of IF low temperature anomalies analogous to those in rolled samples.

3.4.2. Internal friction of hydrogenated $Ni_{60}Nb_{40}$. Figure 10 illustrates the influence of the current density and the hydrogenation time on $Q^{-1}(T)$ and $E(T)$ at fixed ϵ_0 and f. Hydrogenation leads to the appearance of the IF peak and corresponding modulus deficiency. The IF peak height increases with increasing of J and t and the peak shifts to low temperatures. Such a behaviour was pointed out almost in all IF-investigations of hydrogenated MG [9–21].

As it is seen from Fig. 10 the hydrogenation-induced IF peak and the corresponding modulus deficiency are quite similar to those after rolling. Some difference consists of the shift of peak in the low temperature side by 20–50 K and of the absence of low temperature shoulder. However, this shoulder was observed sometimes (see below, Fig. 12). The IF peak in hydrogenated samples just as in rolled specimens is rather stable. 5–6 month exposure at room temperature has little influence on the IF peak height. Modulus deficiencies in hydrogenated and rolled samples are close also.

$Q^{-1}(T)$ and $E(T)$ for the specimen containing 2.6 at.% of hydrogen ($J = 10$ mA/cm^2, $t = 40$ min) at various strain amplitudes are shown in Fig. 11. The regularities in this case are the same as in the rolled samples: an increase of ϵ_0 by an order of magnitude leads to the shift of the peak by ≈ 25 K to low temperatures and to an increase of low temperature damping. IF temperature dependences of the hydrogenated sample at various vibrational frequencies ($\epsilon_0 = \text{constant}$) are shown in Fig. 12. As well as in the case of rolled samples, an increase of f results in a peak shift to high temperatures and in an increase of the peak height, but low temperature damping (at $T < 60$ K) remains practically unchanged. Therefore, one can conclude, just as in the case of rolled samples, that IF has compound character: at temperatures $T < 60$ K hysteresis damping is observed and at higher temperatures hysteresis IF is superimposed by the relaxation peak.

The logarithm of the vibration frequency vs the inverse peak temperature is given by the curve 2 in Fig. 3. The slopes of $\ln f - T^{-1}$ dependences for rolled and hydrogenated samples are the same indicating the same activation energy. The pre-exponential factor for the "hydrogen" peak is, however, considerably smaller and equals $1.7 \cdot 10^{-15}$ s. The evaluation of the activation volume with the help of equation (1) ($T_1 = 230$ K, $T_2 = 212$ K, $\epsilon_{01} = 9 \cdot 10^{-6}$, $\epsilon_{02} = 1.5 \cdot 10^{-4}$, see Fig. 11, $U_0 = 0.51$ eV and $E = 109$ GPa) gives $V = 0.72$ nm^3 what in the b^3-units and in the Ω-units equals about 40 and 80, correspondingly.

The obtained V-value for hydrogenated samples is approximately one fifth of that for rolled samples.

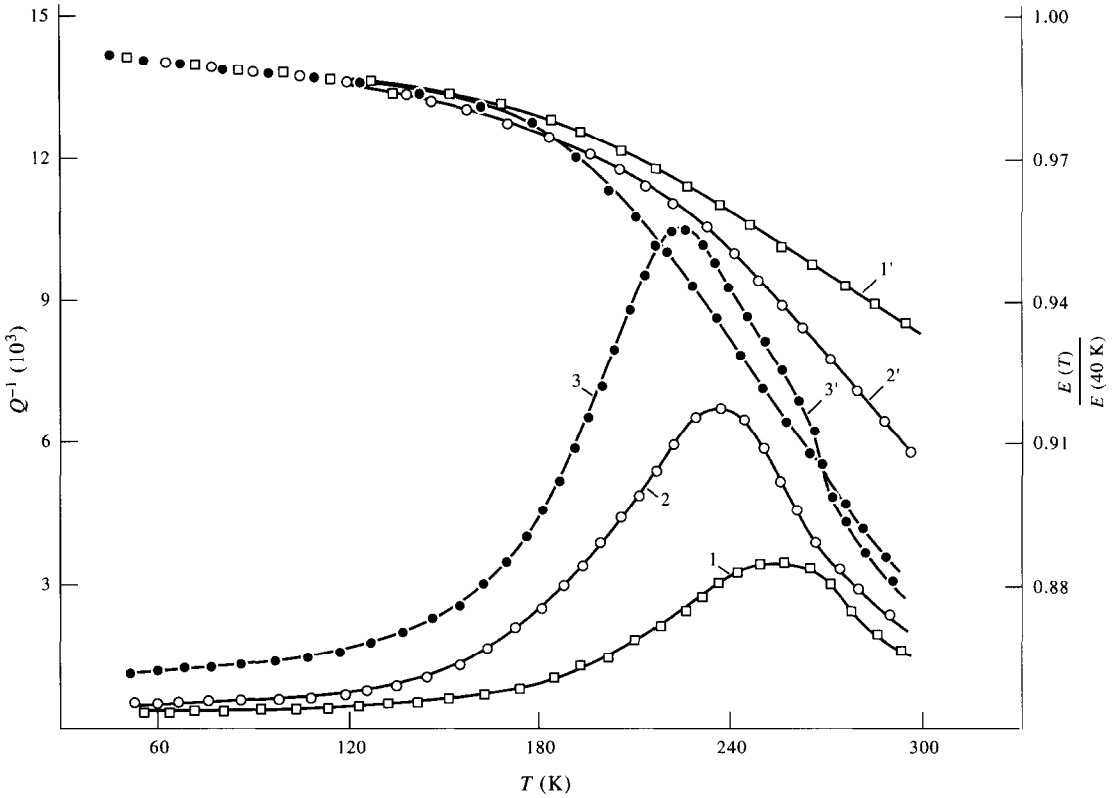

Fig. 10. Temperature dependences of Q^{-1} (1–3) and E (1′–3′) at frequencies ≈ 300 Hz and $\epsilon_0 = 2 \cdot 10^{-5}$ after hydrogenation of samples at $J = 2$ mA/cm^2, $t = 40$ min (1, 1′): $J = 10$ mA/cm^2, $t = 20$ min (2, 2′) and $J = 10$ mA/cm^2, $t = 40$ min (3, 3′).

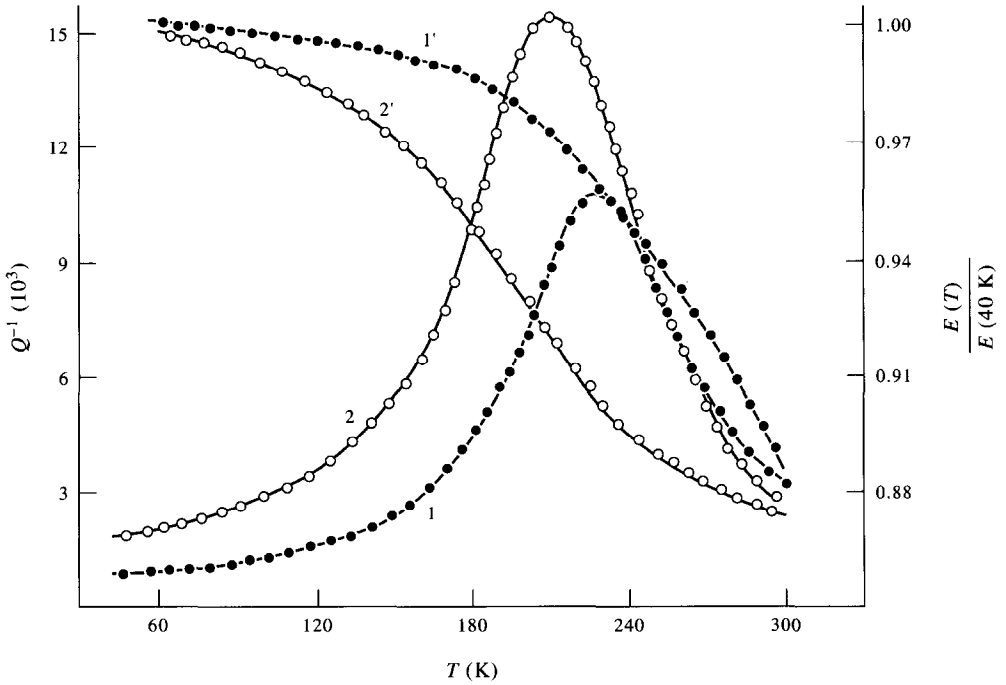

Fig. 11. Temperature dependences of Q^{-1} (1, 2) and E (1′,2′) at frequencies ≈ 300 Hz after hydrogenation of the sample ($J = 10$ mA/cm^2, $t = 40$ min) at $\epsilon_0 = 9 \cdot 10^{-6}$ (1, 1′) and $\epsilon_0 = 1.5 \cdot 10^{-4}$ (2, 2′).

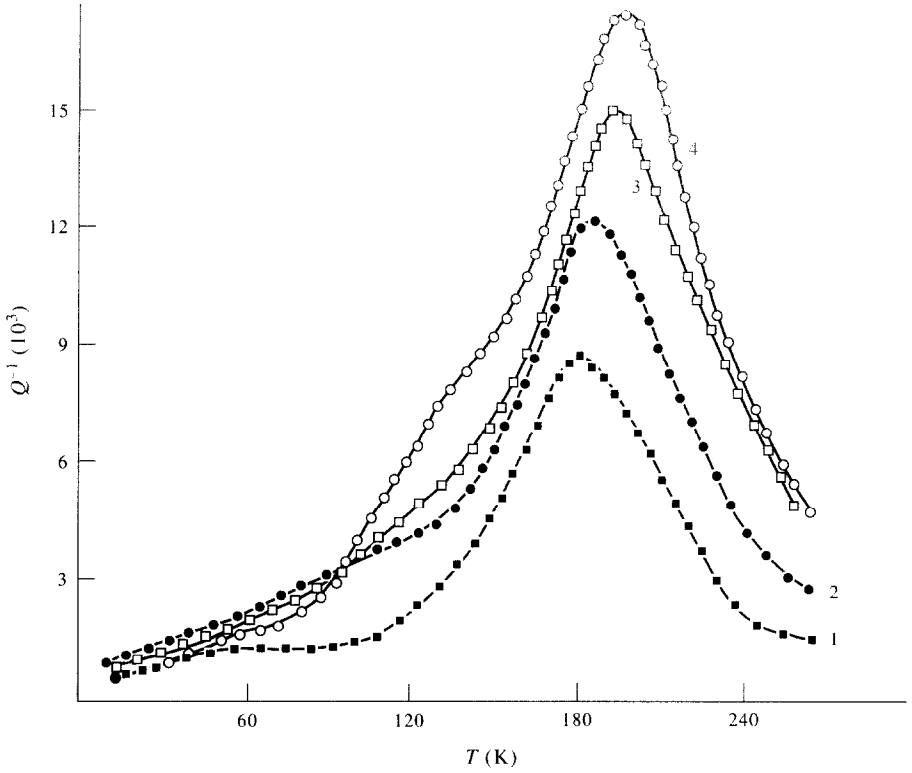

Fig. 12. IF temperature dependences of hydrogenated sample ($J = 10$ mA/cm^2, $t = 20$ min) at various frequencies: 171 (1), 386 (2), 586 (3) and 1486 Hz (4). $\epsilon_0 = 1.9 \cdot 10^{-5}$.

However, it does not change the conclusion about the similarity of the corresponding relaxation processes because the activation volume can have strong stress dependence. According to [40], the activation volume calculated from the stress relaxation data at room temperature for a number of MG decreases from 8 to 10 nm^3 to 1 to 2 nm^3 with an increase of the applied stress. A reduction of V can be a result not only of external stress action but also can be due to an internal stress rise. We believe that lower IF peak temperatures in hydrogenated samples reflect higher internal stresses.

Lowering of the IF peak temperature with increase of the hydrogen concentration, repeatedly mentioned in the literature, can be also treated as a direct consequence of internal stress growth caused by microplastic deformation of structure. The change of the internal shear stress, $\Delta\sigma_s^{int}$, due to the increase of the hydrogenation time by 20 min at $J = 10$ mA/cm^2 [the corresponding $Q^{-1}(T)$ dependences are given by curves 2 and 3 in Fig. 10] can be estimated as follows. Simplifying equation (1) one can write the $\Delta\sigma_s^{int} \approx U_0 \Delta T / TV$, where $\Delta T = T_2 - T_1$ is the change of the peak temperature due to the rise of the internal shear stresses by $\Delta\sigma_s^{int}$, T is the characteristic peak temperature. Taking $T_1 = 235$ K (curve 2, Fig. 10), $T_2 = 214$ K (curve 3, Fig. 10), $\Delta T = 21$ K, $T = (T_1 + T_2)/2$, $V = 0.72$ nm^3 we obtain $\Delta\sigma_s^{int} \approx$ 11 MPa. This result is in good agreement with Fig. 11 data (curves 1 and 2). Indeed, it follows from these data that the decrease of the peak temperature by $\Delta T = 18$ K is due to the increase of the applied shear stress by $\Delta\sigma_s = E\Delta\epsilon_0/\sqrt{3} \approx 9$ MPa. It should be emphasized also that the difference between pre-exponential factors of rolled and hydrogenated samples can have a simple explanation. The activation volume of microplastic flow in MG increases approximately linearly with temperature rise at $T \leqslant 300$ K (just as in the case of crystalline metals at low temperatures [46]): $V = V_0 + \alpha T$ [65]. This fact is the origin of strong pre-exponential factor stress dependence. Indeed, the expression for the relaxation time in this case can be rewritten as $\tau = \tau_0^* \exp((U_0 - \sigma_s V_0)/kT)$, where $\tau_0^* = \tau_0 \exp(-\sigma_s \alpha / k)$. The quantity σ_s includes both external and internal stresses: $\sigma_s = (\sigma_s^{int})_H + (\sigma_s^{ext})_H$. Let us assume, according to our experiments (see above), that $(\sigma_s^{ext})_H = (\sigma_s^{ext})_R$ and $(\sigma_s^{int})_H - (\sigma_s^{int})_R \approx 5$–7 MPa, where the indexes "H" and "R" denote hydrogenated and rolled samples, correspondingly. α for MG can be taken as $\alpha \sim 10^{-2}$ nm^3/K [65]. Then one obtains $(\tau_0^*)_R / (\tau_0^*)_H \approx 10^2$, in agreement with the experimental data (Fig. 3).

Figure 13 illustrates the influence of electron irradiation on $Q^{-1}(T)$ and $E(T)$ of the sample containing 2.6 at.% of hydrogen. The experimental procedure was identical to that described for rolled samples. As can be seen, the irradiation dose of $1 \cdot 10^{19}$ cm^{-2} results in approximately twofold decrease of the IF peak height. Hydrogenated

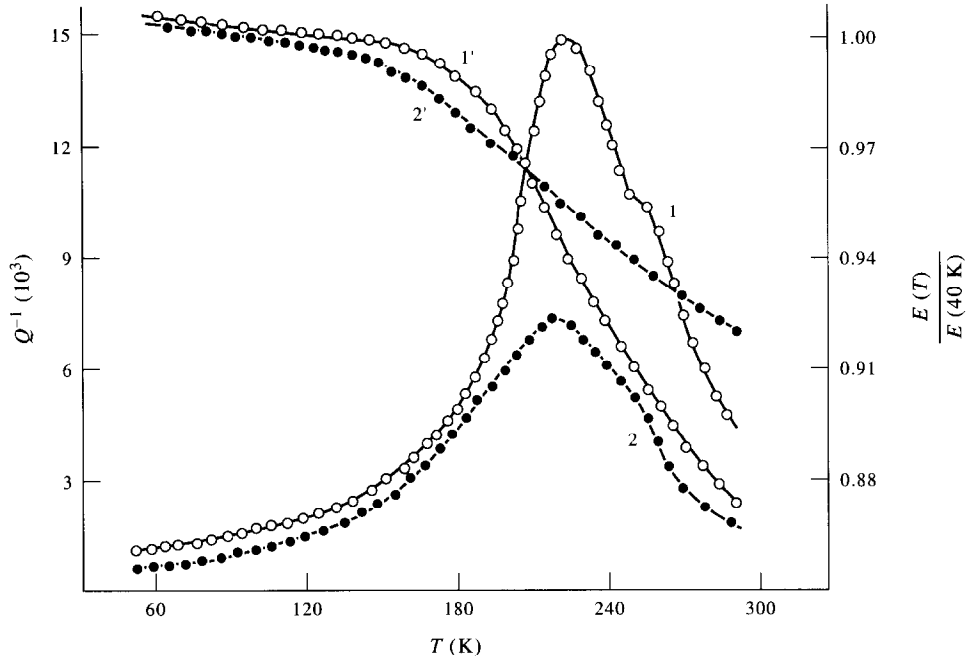

Fig. 13. Influence of 2 MeV electron irradiation on temperature dependences of Q^{-1} (1, 2) and E (1′,2′) of hydrogenated sample at $f \approx 300$ Hz and $\epsilon_0 = 5 \cdot 10^{-5}$: $Q^{-1}(T)$ and $E(T)$ after hydrogenation ($J = 10$ mA/cm^2, $t = 40$ min) (1, 1′) and subsequent $1 \cdot 10^{19}$ cm^{-2} irradiation dose (2, 2′).

samples are less sensitive to irradiation than rolled specimens.

The results considered above show that $Q^{-1}(T)$ and $E(T)$ of rolled and hydrogenated samples are quite analogous. The only phenomenon we have not observed in hydrogenated samples and which, according to the determined analogy must take place, is a decrease of IF peak height at large hydrogen concentrations. However, in the literature this phenomenon is described [14, 16, 23].

Let us consider the influence of the hydrogen-induced microplasticity effect on low temperature IF. Curves 1, 1′ in Fig. 14 show $Q^{-1}(T)$ and $E(T)$ of the sample hydrogenated at $J = 2$ mA/cm^2 during

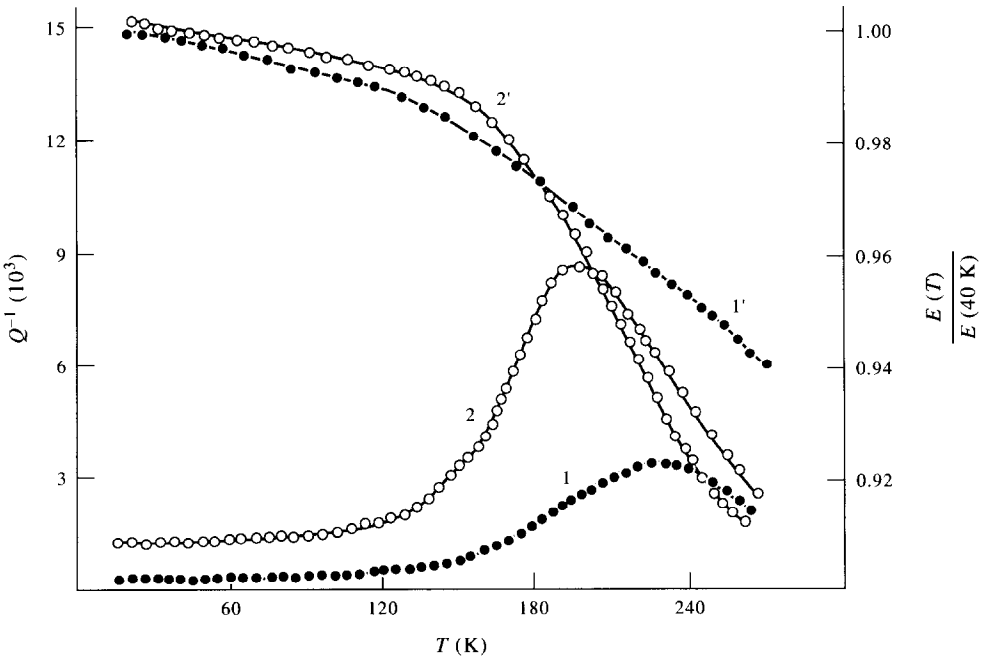

Fig. 14. Temperature dependences of Q^{-1} (1, 2) and E (1′,2′) ($f \approx 300$ Hz, $\epsilon_0 = 5 \cdot 10^{-6}$) after hydrogenation ($J = 2$ mA/cm^2, $t = 40$ min) (1, 1′) and after hydrogenation at the same conditions but in the presence of external tensile stress which caused 2.2% plastic elongation (2, 2′).

$t = 40$ min. The IF peak height under these conditions equals approximately $3.5 \cdot 10^{-3}$ (see also curve 1 in Fig. 10). Curves 2, 2′ represent the corresponding dependences for the sample hydrogenated at the same conditions (current density and time) but in the presence of a tensile load which caused plastic elongation of about 2.2%. It follows from Fig. 14 that hydrogenation-induced microplastic deformation results in three times increase of the IF peak height and in an increase of the corresponding modulus deficiency. This experiment clearly indicates the unity of nature of the deformation and the "hydrogen" IF peaks. The observed displacement of the IF peak to low temperatures after hydrogenation in the stressed state should be attributed to an internal stress rise.

Thus, the experiments and the analysis considered above indicate that the origin of IF peak in MG after hydrogenation is not a Snoek-type relaxation. This conclusion, however, should not be considered as a new one. Indeed, the fundamental possibility of existence of the Snoek relaxation in crystalline metals was questioned as early as in [49, 60, 66] (see also [41]). The grounds for these doubts followed from some experimental data which indicated that displacement fields around dissolved hydrogen atoms should have a symmetry close to the cubic one. Various relaxation processes which occur in crystalline metals after hydrogenation are, most probably, either due to reorientation of hydrogen-impurity complexes or connected with injection of fresh dislocations during hydrogenation and any attempts to obtain reliable identification of these processes as Snoek relaxation failed [41, 60, 61, 66]. At the same time the facts of plastic deformation and dislocation density increase after hydrogenation of crystals are determined in a unique fashion [61, 62]. The results considered above indicate that plastic deformation during MG hydrogenation takes place as well and we believe that it is responsible for the observed anelastic anomalics.

Finally, the following has to be pointed out. Similar IF peaks are observed after hydrogenation of metallic glasses and brittle intermetallic phases obtained by crystallization of amorphous samples [12, 18, 22]. It can be argued that a dislocation relaxation mechanism is unacceptable in this case. However, one must remember that an absence of macroscopic flow does not mean a lack of microplasticity. For example, silicon single crystals which are absolutely macroscopically brittle at room temperature display a wide spectrum of dislocation relaxations even at lower temperatures (see [67] and references therein). We believe that the similarity of relaxation processes in deformed or hydrogenated MG and in crystalline phases of the same composition reflects the similarity of underlying deformation mechanisms.

In conclusion, the whole totality of the obtained results allows us to assert that the observed low temperature anelastic anomalies in the "as-cast", hydrogenated and cold worked MG are due to plastic deformation of structure. Inhomogeneous plastic flow of glassy structure results in formation of dislocation-like defects and motion of these defects under external sign-alternating stress fields causes the $Q^{-1}(T)$ and $E(T)$ peculiarities considered above.

Acknowledgements—The authors are grateful to the late Professor A. M. Rotschupkin, Professor V. I. Belyavskii and Dr A. E. Gol'ter for helpful remarks and discussions. We would like also to thank the Referee for the stimulating criticism.

REFERENCES

1. M. Barmatz and H. S. Chen, *Phys. Rev.* **9,** 4073 (1974).
2. H. N. Yoon and A. Eisenberg, *J. Non-Cryst. Sol.* **29,** 357 (1978).
3. B. S. Berry, W. C. Pritchet and C. C. Tsuei, *Phys. Rev. Lett.* **41,** 410 (1978).
4. H. U. Künzi, K. Ageyman and H.-J. Günterodt, *Solid State Commun.* **32,** 711 (1979).
5. Yu. E. Kalinin and I. V. Zolotukhin, *Fizika tverd. Tela* **22,** 223 (1980).
6. H. U. Künzi, E. Ambruster and K. Ageyman, *Conf. Met. Glass: Sci. Technol. Budapest* **1,** 107 (1981).
7. H.-R. Sinning, E. Wold and F. Haessner, *Mater. Sci. Engng* **97,** 501 (1988).
8. I. V. Zolotukhin and Yu. E. Kalinin, *Fizika Khim. Stekla* **N4,** 663 (1991).
9. B. S. Berry and W. C. Pritchet, *Rapid. Quench. Metals III, London* **2,** 21 (1978).
10. B. S. Berry and W. C. Pritchet, *Scripta metall.* **15,** 637 (1981).
11. B. S. Berry and W. C. Pritchet, *Phys. Rev. B* **24,** 2299 (1981).
12. O. Yoshinary, M. Koiwa, A. Inoue and T. Masumoto, *Acta metall.* **31,** 2063 (1983).
13. K. Kawamura, A. Imai and K. Hiramatsu, *Trans. Jap. Inst. Metals* **24,** 88 (1983).
14. L. E. Hazelton and W. L. Johnson, *J. Non-Cryst. Solids,* **61–62,** 667 (1984).
15. U. Stolz, M. Weller and R. Kirchheim, *Scripta metall.* **20,** 1361 (1986).
16. H. Mizubayashi, Y. Katoh and S. Okuda, *Phys. status solidi* **104,** 469 (1987).
17. I. V. Zolotukhin, Yu. E. Barmin and A. S. Soloviev, *Fizika Metall.* **67,** 201 (1987).
18. B. S. Berry and W. C. Pritchet, *Z. Phys. Chem.* **2,** 381 (1989).
19. H. Mizubayashi, H. Agari and S. Okuda, *Z. Phys. Chem.* **163,** 391 (1989).
20. S. He, Liu M. and L. Taug, *J. Sichuan Univ. Nat. Sci.* **26,** 437 (1989).
21. H.-R. Sinning, M. Nicalaus and F. Haessner, *Scripta metall.* **23,** 471 (1989).
22. H.-R. Sinning, *J. Phys.: Condens. Matt.* **3,** 2005 (1991).
23. H.-R. Sinning, *Phys. status solidi* (a) **140,** 97 (1993).
24. H.-R. Sinning, *J. Alloys Comp.* **211/212,** 216 (1994).
25. I. V. Zolotukhin, V. I. Belyavskii and V. A. Khonik, *Fizika tverd. Tela* **27,** 1788 (1985).
26. V. I. Belyavskii, V. A. Khonik and T. N. Ryabtseva, *Metallofizika* **11,** 106 (1989).
27. I. V. Zolotukhin, V. I. Belyavskii, V. A. Khonik and T. N. Ryabtseva, *Fizika Metall.* **68,** 185 (1989).
28. I. V. Zolutukhin, V. I. Belyavskii, V. A. Khonik and T. N. Ryabtseva, *Phys. status solidi* (a) **116,** 255 (1989).
29. V. A. Khonik, I. A. Safonov and T. N. Ryabtseva, *Fizika tverd. Tela* **9,** 2568 (1992).
30. V. A. Khonik, *J. Alloys Comp.* **211/212,** 114 (1994).

31. M. R. J. Gibbs and J. E. Evetts, *Scripta metall.* **14,** 63 (1980).
32. J. J. Gilman, *J. appl. Phys.* **44,** 675 (1973).
33. J. C. M. Li, *Metall. Trans.* **16A,** 2227 (1985).
34. Yu. A. Skakov and M. V. Finkel, *Izv. VUZov. Tchern. Metall.* **N9,** 84 (1986).
35. V. Lakshamanan and J. C. M. Li, *Mater. Sci. Engng* **98,** 483 (1988).
36. V. S. Boiko, L. F. Krivenko, O. V. Tchernyj and A. M. Bovda, *Fizika tverd. Tela* **30,** 2841 (1988).
37. V. A. Khonik and T. N. Ryabtseva, *Metallofizika* **9,** 52 (1987).
38. V. A. Kuzmitschev, I. V. Zolutukhin, A. T. Kosilov, V. A. Khonik and G. A. Dzuba, *Fizika tverd. Tela* **32,** 722 (1990).
39. I. V. Zolutukhin, A. T. Kosilov, V. A. Khonik, T. N. Ryabtseva, A. A. Lukin and G. F. Prokoshina, *Fizika tverd. Tela* **32,** 1378 (1990).
40. A. T. Kosilov, V. A. Khonik and T. N. Ryabtseva, *Metallofizika* **12,** 37 (1990).
41. V. P. Aliokhin and V. A. Khonik, in *Structure and Physical Regularities of Deformation of Amorphous Alloys*, 248 pp. Metallurgiya, Moskva (1992).
42. A. S. Nowick and B. S. Berry in *Anelastic Relaxation in Crystalline Solids*. Academic Press, New York (1972).
43. A. I. Drojjin, I. V. Sidelnikov and V. S. Postnikov, *Fizika tverd. Tela* **17,** 2417 (1975).
44. M. Koiwa and R. R. Hasiguti, *Acta metall.* **13,** 1219 (1965).
45. E. Swab, Gy. Meszaros, G. Kanezcs, S. N. Ishmaev, S. L. Isakov, I. P. Sadikov and A. A. Chernyshov, *J. Non-Cryst. Solids* **2–3,** 291 (1988).
46. V. I. Startsev, V. Ya. Il'itchev and V. V. Pustovalov, in *Plasticity and Strength of Metals at Low Temperatures*. Metallurgiya, Moskva (1975).
47. V. A. Khonik, A. T. Kosilov, V. A. Kuzmitschev and G. A. Dzuba, *Acta metall. mater.* **40,** 1387 (1992).
48. G. A. Dzuba, I. V. Zolotukhin, Kosilov A. T. and Khonik V. A., *Fizika tverd. Tela* **33,** 3393 (1991).
49. H. Peisl, in *Hydrogen in Metals—I. Basic Properties*, pp. 69–93. Mir, Moskva (1981).
50. A. J. Maeland, *Rapid Quench. Metals Proc. 5th Int. Conf. Wurzburg* **II,** 1507 (1985).
51. S. P. Timoshenko and J. Gudier, in *Theory of Elasticity*, p. 319. Nauka, Moskva (1975).
52. R. D. K. Misra and D. Akhtar, *Mater. Lett.* **3,** 500 (1985).
53. H. Hagi, Y. Hayashi and N. Ohtani, *J. Soc. Mater. Sci.* **44,** 1440 (1980).
54. C. Park, K. Shin, J. Niagakawa and M. Meshii, *Scripta metall.* **14,** 279 (1980).
55. H. Hagi, H. Kajikawa and Y. Hayashi, *J. Soc. Mater. Sci.* **38,** 94 (1989).
56. L. V. Spivak and N. E. Skryabina, *Izv. AN SSSR. Metall.* **N3,** 147 (1988).
57. L. V. Spivak, N. E. Skryabina, L. D. Kurmaeva and L. V. Smirnov, *Fizika Metall.* **66,** 1177 (1988).
58. L. V. Spivak and N. E. Skryabina. *Izv. VUZov. Tchern. Metall.* **N6,** 70 (1988).
59. L. V. Spivak, M. Ya. Katz and N. E. Skryabina, *Fizika Metall.* **N6,** 142 (1991).
60. C. Wert, in *Hydrogen in Metals—II. Application-oriented Properties*, pp. 362–392. Mir, Moskva (1981).
61. P. V. Gel'd, R. A. Ryabov and E. S. Kodes, in *Hydrogen and Structural Imperfections of Metals*, 219 pp. Metallurgiya, Moskva (1979).
62. B. A. Kolatchev, in *Hydrogen Brittleness of Metals*, 217 pp. Metallurgiya, Moskva (1985).
63. A. E. Gol'ter and A. M. Rotschupkin, *Metallofizika* **8,** 60 (1986).
64. M. V. Belous, Yu. A. Kunitsky, A. V. Nemirovsky and V. F. Peklun, *Metallofizika* **11,** 72 (1989).
65. O. P. Bobrov, I. A. Safonov and V. A. Khonik, *Fizika tverd. Tela* **36,** 1703 (1994).
66. A. E. Gol'ter, Cand. Sc. Thesis, 143 pp. Polytechn. Inst., Voronezh (1983).
67. S. A. Antipov, A. I. Drojjin, I. V. Mishin and A. M. Rotschupkin, *Z. Tekhnitch. Fiziki* **59,** 169 (1989).